

General Disclaimer

One or more of the Following Statements may affect this Document

- This document has been reproduced from the best copy furnished by the organizational source. It is being released in the interest of making available as much information as possible.
- This document may contain data, which exceeds the sheet parameters. It was furnished in this condition by the organizational source and is the best copy available.
- This document may contain tone-on-tone or color graphs, charts and/or pictures, which have been reproduced in black and white.
- This document is paginated as submitted by the original source.
- Portions of this document are not fully legible due to the historical nature of some of the material. However, it is the best reproduction available from the original submission.



Technical Memorandum 85094

SOLAR RADIO BURST AND IN SITU DETERMINATION OF INTERPLANETARY ELECTRON DENSITY

(NASA-TM-85094) SOLAR RADIO BURST AND IN SITU DETERMINATION OF INTERPLANETARY ELECTRON DENSITY (NASA) 28 p HC A03/MF A01

N83-35989

CSCL 03B

G3/93

Unclassified
42134

J. L. Bougeret, J. H. King

and R. Schwenn

September 1983



National Aeronautics and Space Administration

Goddard Space Flight Center
Greenbelt, Maryland 20771

SOLAR RADIO BURST AND IN SITU DETERMINATION
OF INTERPLANETARY ELECTRON DENSITY

J.-L. Bougeret (*), J.H. King,

Laboratory for Extraterrestrial Physics,
NASA/Goddard Space Flight Center,
Greenbelt, Maryland 20771, U.S.A.

and R. Schwenn

Max-Planck-Institut für Aeronomie,
Postfach 20, D-3411 Katlenburg-Lindau,
Federal Republic of Germany

(*) NAS/NRC Postdoctoral Research Associate on leave from Laboratory
Associated with CNRS # 264, Paris Observatory, France.

to be submitted to: Solar Physics

ABSTRACT

We review and discuss a few interplanetary electron density scales which have been derived from the analysis of interplanetary solar radio bursts, and we compare them to a model derived from 1974-1980 Helios 1 and 2 in situ density observations made in the 0.3-1.0 AU range. The Helios densities were normalized to 1976 with the aid of IMP and ISEE data at 1 AU, and were then sorted into 0.1 AU bins and logarithmically averaged within each bin. The best fit to these 1976-normalized, bin averages is $N(R_{AU}) = 6.1 R^{-2.10} \text{ cm}^{-3}$. This model is in rather good agreement with the solar burst determination if the radiation is assumed to be on the second harmonic of the plasma frequency. This analysis also suggests that the radio emissions tend to be produced in regions denser than the average where the density gradient decreases faster with distance than the observed $R^{-2.10}$.

INTRODUCTION

Even though the solar corona and interplanetary medium are known to be strongly inhomogeneous, average models are sometimes helpful. So are the electron density models needed by solar radioastronomers. Indeed, many of the solar radio emissions are directly related to the plasma frequency f_p in the source region: $f_p = 9 N^{1/2}$ (f_p , Hz and N : electron number density, m^{-3} ; or f_p , kHz and N , cm^{-3}). It follows that knowledge of the density model yields the source distance from the Sun and hence the speed of a traveling disturbance (electron packet for a type III burst, shock wave for a type II burst, see Wild and Smerd, 1972). Conversely the radio observation can provide a remote measurement of the density at the source location, which is of particular interest if the source position can be measured separately.

Solar corona electron density distributions have been deduced from coronal photometric and polarization data, from radio source solar occultations, from the measurement of the angular deflection of signals from distant radio sources, from the measurement of the radio frequency dispersion of the signals from pulsars, and from the analysis of single and dual frequency time delay data acquired from interplanetary spacecraft (see e.g. Esposito *et al.*, 1980). Such methods usually give access to the solar corona up to a few tens of solar radii (r_\odot).

By contrast with these latter methods which integrate the studied effect along the line-of-sight, the solar radio burst methods discussed below yield density estimates in remote but localized radio emission source regions. Furthermore, the medium can be studied only along the stucture or trajectory

where the radio emission is produced. Such techniques enable one to describe, by remote sensing, the distance range from the base of the solar corona to 1 AU, though most observations yield models which are only valid over a shorter range of distances.

The derivation of electron density distributions from the observation of solar radio bursts has been frequently discussed in the past for ground-based radio observations from decimeter to decameter wavelengths (Wild *et al.*, 1963; Malitson and Erickson, 1966; Wild and Smerd, 1972; Mercier and Rosenberg, 1974; Stewart, 1976). These wavelengths give access to heliocentric distances ranging from the base of the solar corona up to $2-3 R_{\odot}$. The results are summarized in Fig. 1 (curve 4) by a curve taken from Malitson and Erickson (1966), which is still in very good agreement with the present day radioheliograph observations.

In this paper, we review density distributions deduced from solar radio burst observations from satellites and spacecraft on hectometer and kilometer wavelengths which give access to the interplanetary medium from a few R_{\odot} up to 1 AU. We then compare those density distributions to a density model derived from the Helios 1 and 2 in situ density observations.

SOLAR RADIO BURST ELECTRON DENSITY SCALES IN THE INTERPLANETARY MEDIUM

Interplanetary type III solar radio bursts and more rarely type II bursts have been used to derive electron density distributions. These bursts are characterized by a narrow band of radio emission about the local plasma

frequency and/or its second harmonic at coronal and interplanetary levels of decreasing density. Until the mid 70's, most authors hypothesized a type III burst radiation on the fundamental of the plasma frequency. The most recent type III theories (Smith et al., 1979) and a number of observational evidences support a radiation on the second harmonic (Fainberg and Stone, 1974; Gurnett et al., 1978). The emission of the harmonic instead of the fundamental would result in an overscaling of the densities deduced from the radio burst observations by a factor of 4. We show in Figure 1a density scales which assume radiation at the fundamental, and in Figure 1b we have applied this ratio of 4. We will discuss the fundamental/ harmonic problem in more detail in the last section. For comparison, we show in Fig. 1 (curve 1) the Newkirk's (1967) model scaled for solar maximum.

Following Alvarez and Haddock (1973), we shall use the following expression for the density:

$$N(r) = A (r-b)^p \quad (1).$$

Alvarez and Haddock have shown that this formula can describe with good accuracy coronal and interplanetary density models in a large range of heliocentric distances. Formula (1) describes a power law falloff at large r (i.e. $r \gg b$), but allows an even steeper dependence on r very close to the Sun. Table 1 summarizes the values of p , b and A for some of the observations discussed below.

Early hectometer and kilometer wavelength observations of radio bursts from satellite (Hartz, 1964; Slysh, 1967a,b,c) already suggested that the radio sources were much more distant from the Sun than could be accounted for by the extrapolation of the existing coronal density models.

Hartz (1969) (curve 5 in Fig. 1; Table 1) used radio data from the Alouette I and II satellites in the range from 0.1 MHz to 15 MHz. The interpretation of the decay rates and average source drift velocities led Hartz to an electron density model whose values exceeded the average solar wind densities by about an order of magnitude.

Alexander et al. (1969) (curves 6-I and 6-II in Fig. 1; Table 1) used type III radio bursts observed from 3000 to 450 kHz with the ATS-II satellite to derive two alternative density models of active region streamer in the outer corona, assuming pressure equilibrium. Model I uses streamer electron temperatures derived by assuming a collisional damping decay of the bursts. The temperatures thus deduced are lower than the average coronal temperature, allowing higher densities in the streamer. In model II the streamer electron temperature is assumed to equal the average coronal temperature. In that case the burst decay is interpreted by Landau damping, as later proposed by Harvey and Aubier (1973). Alexander et al. suggest that actual streamer parameters fall somewhere between these limits. We note that these limits almost include the Newkirk's maximum model if the harmonic is assumed (Fig. 1b), and that the power law indices of the two extreme models vary between -2.5 and -3.3.

Fainberg and Stone (1971) (curve 7 in Fig. 1; Table 1) have deduced from the analysis of a type III storm a density model in the range 10-40 solar radii (sometimes referred to as the RAE model). It is closely approximated by a power law of the form : $N=5.52 \cdot 10^7 r^{-2.63}$ (N , cm^{-3} ; r , R_\odot), or $N=40 R^{-2.63}$ (N , cm^{-3} ; R , AU). In these units the coefficient is the extrapolated density at 1 AU). However, this technique provides only the level separation between different frequencies. The absolute distance of one of the plasma levels had

to be fixed. This free parameter was adjusted so that the exponent of R in the model was close to that of Newkirk's (1967) quiet sun model.

Malitson et al. (1973) analyzed a type II solar radio burst which was associated with a 3B flare and was observed down to 30 kHz (near 1 AU) by the radio astronomy experiment on the IMP-6 satellite. The occurrence of a sudden-commencement geomagnetic storm and the time of the flare set narrow limits on the average true shock velocity in the interplanetary medium. Henceforth a frequency scale can be deduced, from which the density scale is obtained. This density scale is in remarkably good agreement with the RAE density scale provided the type III storm burst emission is observed at the second harmonic of the plasma frequency. The observation cannot be accounted for if the fundamental is assumed. This is consequently regarded as a strong evidence for a type III radiation on the second harmonic.

Alvarez and Haddock (1973) (curve 8 in Fig. 1; Table 1) have shown that the frequency drift rate of the type III bursts can be fitted with a remarkable accuracy to: $df/dt = -0.01 f^\alpha \text{ MHz s}^{-1}$ over a very wide range of frequencies. Between 550 MHz and 75 kHz $\alpha = 1.84 \pm 0.02$, and for the low frequency OGO-5 data reported (between 3500 kHz and 50 kHz) $\alpha = 1.93 \pm 0.05$. This expression and some simplifying assumptions enable them to obtain the empirical formula (1) for the electron density distribution in the solar wind, where $p = -2/(\alpha-1)$. The parameter A in (1) is best determined by the electron density observed at 1 AU, $N(215)$. The parameter b is best determined by the electron density near the Sun, $N(1)$. The parameter p which is the power law index of the density distribution, is quite well determined by the observation of the frequency drift rates. For the full frequency domain, the average index

is $p = -2.38 \pm 0.05$. For the low frequency data alone, which describe the interplanetary medium, $p = -2.15 \pm 0.11$. This value is valid for frequencies between about 3 MHz and 75 kHz. Assuming a type III radiation on the second harmonic, this approximately corresponds to a distance range between about 5 R_{\odot} and 180 R_{\odot} . We note that this model is in remarkably good agreement with Hartle and Sturrock's (1968) theoretical two-fluid model of the solar wind, when the densities of the solar wind at 1 AU are equated. The curve shown in Fig. 1 is normalized to the 1 AU Helios density which will be discussed later (6.14 cm^{-3}).

Davis and Feynman (1977) discuss interplanetary density models in their analysis of a type II radio burst. They suggest that, for undisturbed conditions the density may be expected to vary as $R^{-2.4}$ for $R \leq 40 R_{\odot}$, and that for $R > 100 R_{\odot}$ the average variation is probably close to R^{-2} . They also note that the density models derived from type III bursts may apply to solar wind density structures which evolve in stream interaction regions.

Gurnett et al. (1978) (squares 2 in Fig. 1; Table 1) determined the three-dimensional trajectory of a type III burst using stereoscopic direction finding measurements from the IMP 8, Hawkeye 1, and Helios 2 spacecraft. By comparing the observed source positions with the direct in situ solar wind density measurements obtained by Helios 1 and 2 near the Sun, they demonstrated that the type III radio emission occurred near the second harmonic of the local plasma frequency for the event they observed.

Stone (1980) (circles in Fig. 1; Table 1) also used a direction finding triangulation technique to derive the trajectory of a type III burst observed

simultaneously from ISEE-3 and Helios 2. He deduced an interplanetary electron density scale between 0.15 AU and 0.75 AU.

Bougeret et al. (1982) (curve 9 in Fig. 1; Table 1) used corotating storms of type III bursts to derive a frequency scale in the range 10-170 R_{\oplus} . Four different storms show different density models, with power law indices in the range from -2.2 to -4. The average model is in good agreement with and extends the previous RAE model by Fainberg and Stone (1971).

THE HELIOS 1 AND 2 PLASMA DENSITY MEASUREMENTS

The analysis of in situ plasma density observations to obtain an average radial density profile is complicated by a number of factors. First of all, short term (hours-days) variability in plasma density requires that long data spans be used. Such long spans are also required to cover an adequate range of heliocentric distance. In order to minimize the chance that peculiarities associated with a single traversal of the heliocentric distance range will yield a misleading density profile, it is desirable to have several such traversals. However, several traversals imply coverage over a significant fraction of a solar cycle. In this case, solar cycle variations in densities must be accounted for, lest they bias the results.

We have used hourly averaged ion density data obtained by the quadrispheric electrostatic analyzers flown on the Helios 1 and 2 spacecraft. See Rosenbauer et al. (1977) for instrumental details. The Helios spacecraft, launched in December 1974 and January 1976, covered the heliocentric distance

range 0.3 to 1.0 AU every 3 months. Our data base extends from spacecraft launch into 1980, thus covering a large number of traversals of the 0.3 - 1.0 AU heliocentric distance regime.

Since this Helios data base spans half a solar cycle, we have sought possible solar cycle density variations in the 1 AU IMP/ISEE data record (King, 1979; 1983). Figure 2 shows annual averages of sunspot number and of ion density at 1 AU, for the years 1974-1980. The density values are geometric averages; that is, owing to the log-normal distribution of hourly density values, arithmetic averages of logarithms of hourly densities were taken. We note that arithmetic density averages are \sim 20-25% greater than the geometric averages shown.

There is a general anticorrelation between sunspot number and interplanetary density, as has been pointed out by previous authors (Diadato et al., 1974; Schwenn, 1983). From Fig. 2 it appears that the sunspot profile leads the anticorrelated interplanetary density profile by one year. It is beyond the scope of this paper to pursue this point.

In order to eliminate solar cycle variations from the Helios data base, we have normalized all data to 1976, when the 1 AU density was near its maximum. That is, each Helios hourly density value obtained during year J has been multiplied by $N(1AU;1976)/N(1AU;Year J)$. For convenience, we refer to these time-normalized Helios densities as simply Helios densities from here on.

All Helios densities were then sorted into 0.1 AU bins, and geometric averages were taken. Figure 3 shows the Helios 1 and 2 averages separately.

The standard deviations in the bin averages of density logarithms ranged between 0.26 and 0.31. The error bar shown in Fig. 3 corresponds to a standard deviation of 0.28. There are between 2000 and 11000 individual hours in each bin average. Allowing for a 12-hr autocorrelation time, we conclude that the standard errors in the means correspond to error bars which are a factor of 10 to 30 smaller than the standard deviation error bar shown. Note that the Helios 1 and 2 bin averages generally agree well with each other. In the 0.4-0.5 AU bin of greatest difference in the means, the means lie well within one standard deviation of each other but somewhat outside the standard error. We attribute no significance to this fact.

A linear least squares fit of $\langle \log N \rangle$ vs $\log R$ yields

$$N(R) = (6.16 \pm 0.15) R^{(-2.12 \pm 0.04)} \quad \text{for Helios 1 and}$$

$N(R) = (6.12 \pm 0.18) R^{(-2.07 \pm 0.05)} \quad \text{for Helios 2. Here } R \text{ is in}$
units of AU and N of cm^{-3} . (Using $\log \langle N \rangle$ instead of $\langle \log N \rangle$ gives powers of -2.14 and -2.08.) The one-sigma uncertainty in the slopes (exponents) is of order 0.04. The corresponding uncertainty in the intercept (in log space) is 0.01. Thus a density model which well represents the 0.3-1.0 AU Helios density data taken over 1974 to 1980, but normalized to 1976, is

$$N(R_{\text{AU}}) = 6.14 R^{-2.10} \text{ cm}^{-3} \quad (2)$$

This model is shown on Figure 1 (curve 10). Note that the Helios 1 AU, 1976 density value of 6.14 cm^{-3} is significantly less than the corresponding 1976 IMP density shown in Fig. 2. This is consistent with Schwenn's (1983) finding that Los Alamos IMP densities (to which all densities of the IMP/ISEE compilation have been normalized) must be multiplied by 0.7 to make them

consistent with the Helios densities observed near launch. Schwenn (1983) also found his absolute density calibration good to within 20%, by comparison with measurements of the electron plasma frequency associated with strong plasma oscillation. This 20% relates to the absolute accuracy in the Helios density model, whereas the previously cited 0.01 uncertainty in the log-density intercept relates only to statistical (or relative) uncertainties in the model.

DISCUSSION AND CONCLUSION

The Helios density model

We have deduced from the analysis of 1974-1980 Helios 1 and 2 in situ density observations the density model $N(R_{AU}) = 6.1 R^{-2.10} \text{ cm}^{-3}$. This model is valid over the range 0.3 AU to 1 AU and is normalized to 1976, when the 1 AU density is near its maximum. The power law index (-2.10 ± 0.04) shows evidence for a deviation from the R^{-2} dependence expected for a steady, spherically symmetric solar wind expansion. This result is in good agreement with Schwenn's (1983) who used a quite different approach. Schwenn used arithmetic averages while we used geometric, and he used finer bin resolution and time resolution. He investigated the radial variation of the average proton density between 0.3 AU and 1 AU, in per cent, as compared to a R^{-2} dependence. His findings of -18.1% for Helios 1 and -10.1% for Helios 2 can be converted respectively in power law indices of -2.14 and -2.08 , to be compared to our values of -2.12 ± 0.04 and -2.07 ± 0.05 respectively for Helios 1 and 2. This decrease in density from 0.3 AU to 1 AU is consistent with the increase in the average velocity V found by Schwenn (1983): the average flux ($N V R^2$) remains

constant. This average model is thus consistent with a spherically symmetric flow with a slight acceleration of the average solar wind between 0.3 AU and 1 AU. The general anticorrelation between sunspot number and interplanetary density that we deduced from IMP/ISEE 1 AU observations is consistent with that found by Schwenn (1983) who used Helios 1 and 2 data alone.

Fundamental and second harmonic hypotheses

We have reviewed solar radio burst determinations of the electron density distribution in the solar wind, in regions where other remote sensing methods provide sparse information. The radio burst techniques are generally based on the observation of type III radio bursts. They provide higher densities than the *in situ* Helios model. An interpretation of this discrepancy is that most type III radio bursts are radiated at the second harmonic of the plasma frequency rather than the fundamental in agreement with recent theories (Smith *et al.*, 1979) and some observations (Fainberg and Stone, 1974; Gurnett *et al.*, 1978). This results in the factor 4 already mentioned and applied between Figs. 1a and 1b. However, Melrose (1982) points out that the evidence for radiation at the second harmonic in type III bursts is circumstantial, and that some observations are better explained by a radiation at the fundamental. But such an hypothesis requires the assumption of strong scattering effects -ducting of the radiation from the fundamental level up to a higher level in the corona, close to the level expected in the harmonic hypothesis (Duncan, 1979). Indeed, ground based observations show that, in the rare cases when both fundamental and harmonic are believed to be present, they are almost spatially coincident when observed at the same frequency, while they should be

observed at levels differing by a ratio of 4 in density. We note that this last situation (fundamental and ducting) is equivalent to the first (harmonic) in the determination of density models, since what is important is where the source is observed at a given frequency. As a matter of fact, the conflicting hypotheses can be summarized as follows: either the harmonic is emitted and observed at its true location, or the fundamental is emitted and the radiation has to be ducted up to the harmonic level where it is observed. We conclude that the observed heliocentric distances of the radio sources can be used to infer density models in any of these hypotheses. There is still no clear answer to which mode is observed. Although our inclination is that the second harmonic may be dominant, the occurrence of fundamental emission cannot be ruled out (Kellog, 1980).

Radio burst source sizes

Interplanetary radio burst sources as seen from the Sun can subtend an angle as large as 50° (Bougeret *et al.*, in preparation). Scattering is very likely to contribute significantly to this size. Scattering models have been extensively investigated for the lower corona conditions (Steinberg *et al.*, 1971; Riddle, 1974). The only analysis available for interplanetary conditions (Steinberg, 1972) was made when very little information was available on source sizes in the interplanetary medium. Using ray tracing technique, Hornstein (private communication) finds that the scattered image of a point source observed at 110 kHz and located at 0.5 AU may have an apparent size close to 40° when observed from 1 AU. Hence the true radiation source may have a relatively small extent. Thus, the radio burst observations at a given

frequency are likely to sample a restricted region of the interplanetary medium. However, if scattering is important, its effect in introducing a bias in the radio determination of interplanetary densities is uncertain. Further detailed modeling of the scattering of interplanetary bursts is required to resolve this point.

Radio burst source location

Figure 1b and Table 1 (see extrapolated 1 AU density) clearly show that, even when the harmonic is assumed, the radio densities are still higher than the Helios density model, even though the model is normalized to 1976 when the 1 AU density is near its maximum. This indicates that the radio emissions tend to be produced in regions denser than the average -e.g. streamers. This was already suggested by several authors and convincing observational evidence has recently been presented by Kundu et al. (1983). For the interplanetary medium, Davis and Feynman (1977) suggested that even if type III bursts are produced on any field line near the Sun, then the interactions of high-speed solar wind streams will cause type III bursts to appear preferentially along density enhancements because stream-stream interactions compress magnetic field lines along with the particles. Those restricted regions with enhanced density might well be difficult to detect using conventional (other than in situ) methods. As already mentioned, the radio burst observations provide a local measurement, while the other methods integrate along the line-of-sight, hence averaging irregularities.

The density falloff

The density falloff is a critical parameter in the determination of radio disturbance speeds in the interplanetary medium, since the density scale height depends upon the power law index. Its values are summarized in Table 1. When $b \neq 0$ in (1), the falloff will be steeper closer to the Sun, consistent with the density measurements in the lower corona. We have noted previously that the deviation of the Helios $R^{-2.10}$ dependence from the expected $R^{-2.0}$ -which would apply in the acceleration-free, spherically symmetric situation- may be evidence for extended solar wind acceleration, especially since the particle flux $-N V-$ has been shown elsewhere to have a dependence much closer to $R^{-2.0}$. The falloffs derived from the radio burst observations are generally steeper than the $R^{-2.10}$ Helios density model, which averages over all solar wind conditions. We are unable to uniquely identify the cause of this deviation from the Helios $R^{-2.10}$ dependence. On the one hand, the solar wind may still be accelerating in the enhanced regions where the bursts are produced. On the other hand, these enhanced density regions may be spatially diverging significantly faster than the $R^{-2.0}$ expected in the simplest view. Again the role of scattering has to be clearly understood, especially when the source gets close to the observer (the observer may be inside the scattering region -a case never considered by previous scattering analyses). The major problem remains to exactly know which regions of the solar wind the radio burst analysis samples. Direct analyses of in situ density measurements within the radio burst source location and a thorough understanding of the influence of scattering in the interplanetary medium are certainly needed before the interplanetary radio burst methods can be very accurately used as a common tool to remotely determine the solar wind density. For instance density models

derived from type III burst analysis may be different for storm bursts and flare-related bursts, and may not apply directly to type II bursts. However, we believe that the radio burst method remains a unique possibility of remote analysis of important regions in the interplanetary medium (interplanetary extension of active regions, streamers, stream-stream interaction regions, shocks).

References

Alexander, J.K., Malitson, H.H., and Stone, R.G.: 1969, Solar Phys. 8, 388

Allen, C.W.: 1947, M.N.R.A.S. 107, 426

Alvarez, H.: 1971, UM/RAO Report 71-9, University of Michigan, 62-119

, Alvarez, H., and Haddock, F.T.: 1973 Solar Phys. 29, 197

Bougeret, J.-L., Fainberg, J., and Stone, R.G.: 1982, NASA Technical Memorandum 84946, Greenbelt, Md 20771, USA, submitted to Astron. Astrophys.

Davis, W.D., and Feynman, Joan: 1977, J. Geophys. Res. 82, 4699

Diadato, L., Moreno, G., Signorini, C., and Ogilvie, K.W.: 1974, J. Geophys. Res. 79, 5095

Duncan, R.A.: 1979, Solar Phys. 63, 389

Esposito, P.B., Edenhorfer, P., and Lueneburg, E.: 1980, J. Geophys. Res. 85, 3414

Fainberg, J., and Stone, R.G.: 1971, Solar Phys. 17, 392

Fainberg, J., and Stone, R.G.: 1974, Space Sci. Rev. 16, 145

Gurnett, D.A., Baumback, M.M., and Rosenbauer, H.: 1978, J. Geophys. Res. 83, 616

Hartle, R.E., and Sturrock, P.A.: 1968, Astrophys. J. 151, 1155

Hartz, T.R.: 1964, Ann. Astrophys. 27, 831

Hartz, T.R.: 1969, Planet. Space Sci. 17, 267

Harvey, C.C., and Aubier, M.G.: 1973, Astron. Astrophys. 22, 1

Kellog, P.J.: 1980, Astrophys. J. 236, 696

King, J.H.: 1979, Interplanetary Medium Data Book - Supplement 1, NSSDC 79-08

King, J.H.: 1983, Interplanetary Medium Data Book - Supplement 2, NSSDC 83-01

Kundu, M.R., Gergely, T.E., Turner, P.J., and Howard, R.A.: 1983, Astrophys. J. Lett. (in press)

Malitson, H.H., and Erickson, W.C.: 1966, Astrophys. J. 144, 337

Malitson, H.H., Fainberg, J., and Stone, R.G.: 1973, Astrophys. J. 183, L35

Malitson, H.H., Fainberg, J., and Stone, R.G.: 1976, Space Sci. Rev. 19, 511

Melrose, D.B.: 1982, Solar Phys. 79, 173

Mercier, C., and Rosenberg, H.: 1974, Sol. Phys. 39, 193

Newkirk, G., Jr.: 1967, Ann. Rev. Astron. Astrophys. 5, 213

Riddle, A.C.: 1974, Sol. Phys. 35, 153

Rosenbauer, H., Schwenn, R., Marsch, E., Meyer, B., Miggenreider, H.,
Montgomery, M.D., Mülhäuser, K.H., Pilipp, W., Voges, W., and Zink, S.M.:
1977, J. Geophys. 42, 561

Schwenn, R.: 1983, in Solar Wind Five (in press)

Slysh, V.I.: 1967a, Soviet Astron. AJ 11, 72

Slysh, V.I.: 1967b, Cosmic Res. 5, 759

Slysh, V.I.: 1967c, Soviet Astron. AJ 11, 389

Smith, R.A., Goldstein, M.L., and Papadopoulos, K.: 1979, Astrophys. J. 234,
348

Steinberg, J.-L.: 1972, Astron. Astrophys. 18, 382

Steinberg, J.-L., Aubier-Giraud, M., Leblanc, Y., and Boischot, A.: 1971,
Astron. Astrophys. 10, 362

Stewart, R.T.: 1976, Solar Phys. 50, 437

Stone, R.G.: 1980, in Radio Physics of the Sun, eds. M.R. Kundu and T.E.
Gergely, D. Reidel, 405

Wild, J.P., Smerd, S.F., and Weiss, A.A.: 1963, Ann. Rev. Astron. Astrophys.
1, 291

Wild, J.P., and Smerd, S.F.: 1972, Ann. Rev. Astron. Astrophys. 10, 159

CAPTIONS

Figure 1: Variation of electron density with distance from the center of the Sun. the radio burst models 2 through 7, and 9 assume a radiation on the fundamental of the plasma frequency in (a), and on the harmonic in (b), resulting in a factor of 4 in the densities between (a) and (b), for those models. Models 1, 8, and 10 are the same in (a) and (b).

1: Newkirk maximum (1967)

2: Gurnett et al. (1978)

3: Stone (1980)

4: Malitson and Erickson (1966), as shown in their Figure 4 (still in very good agreement with the present day radioheliographic observations.)

5: Hartz (1969)

6: Alexander et al. (1969), which shows two limiting cases corresponding to different interpretations mentioned in the text.

7: Fainberg and Stone (1971)

8: Alvarez and Haddock (1973): the model shown on this Figure is normalized to the 1 AU Helios density found in this paper (6.14 cm^{-3} .)

9: Bougeret et al. (1982)

10: The Helios density model found in this paper. The error bar shown corresponds to the absolute accuracy of 20% discussed in the text.

Figure 2: Annual averages of sunspot number and of 1 AU density as given by the 1 AU IMP/ISEE data record (King, 1979 ; 1983), for the years 1974-1980. The error bar shown for the 1977 1 AU density gives the standard error in the mean computed with allowance for autocorrelation in the density time series.

Figure 3: Helios 1 and 2 average densities. The error bar shows the typical standard deviation in the bin averages. The standard error of the mean is a factor 10 to 30 smaller.

TABLE 1

Authors	type of measure	range (R_{\odot})	1 AU density (cm^{-3}) ⁺	power law index p	param. b in eq. (1) (R_{\odot})
Hartz, 1969	III B	3-40	30	-2.3	1.0
Alexander <u>et al.</u> , 1969	III B	10-50	25 to 3	-2.5 to -3.3	0.0
Fainberg and Stone, 1971	III S	10-40	10	-2.6	0.0
Alvarez and Haddock, 1973	III B				
	all data	1-180	-	-2.38 ± 0.05	0.95
	OGO-5 only	5-180	-	-2.15 ± 0.11	1.0
Davis and Feynman, 1977	type II	< 40	-	-2.4	-
		> 100	-	-2	-
Gurnett <u>et al.</u> , 1978	III B [*]	86-130	9	-2.5	0.0
Stone, 1980	III B [*]	40-160	10	-2.75 ± 0.18	0.0
Bougeret <u>et al.</u> , 1982	III S	10-170	10	-2.8 ± 0.7	0.0
This paper (Helios)	in situ	65-215	6.14	-2.10 ± 0.04	0.0

type of measure: III B = type III bursts

III S = type III storms

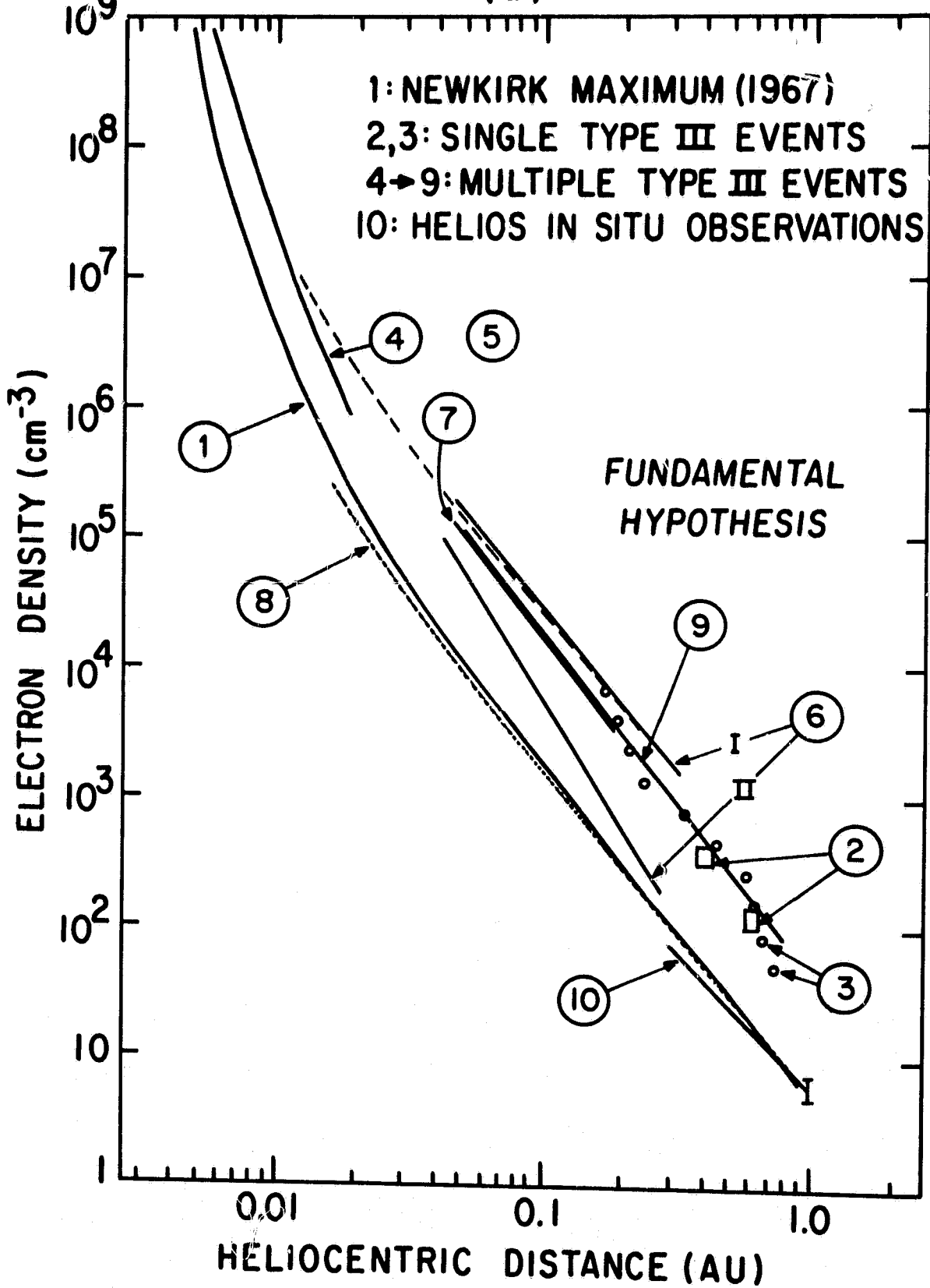
* = single burst analysis. Number of frequency levels

measured: Gurnett et al. (2); Stone (10).

(+): the extrapolated 1 AU density (cm^{-3}) assumes radiation at the harmonic

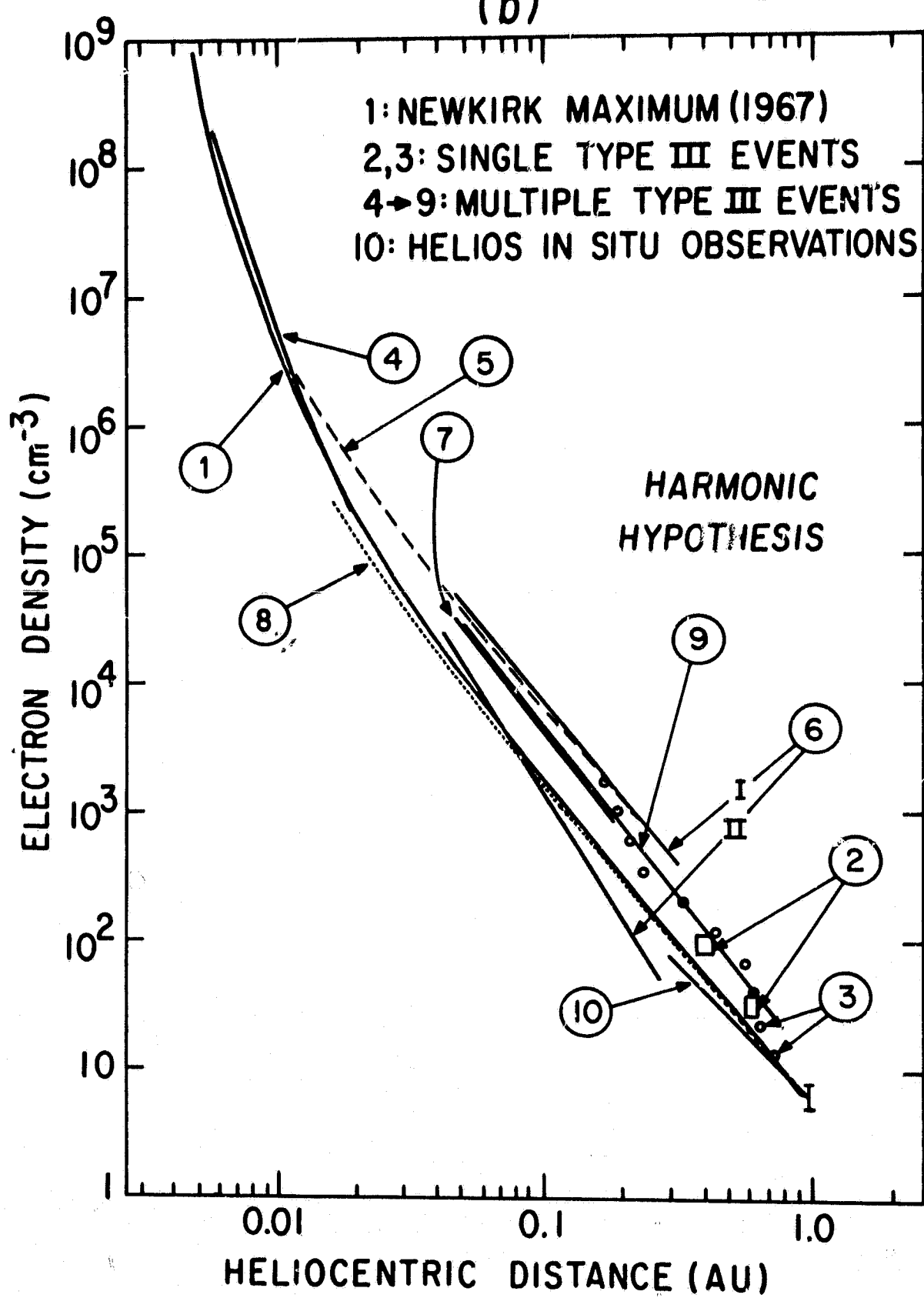
(a)

Figure 1a



(b)

Figure 1b



ORIGINAL PAGE IS
OF POOR QUALITY

Figure 2

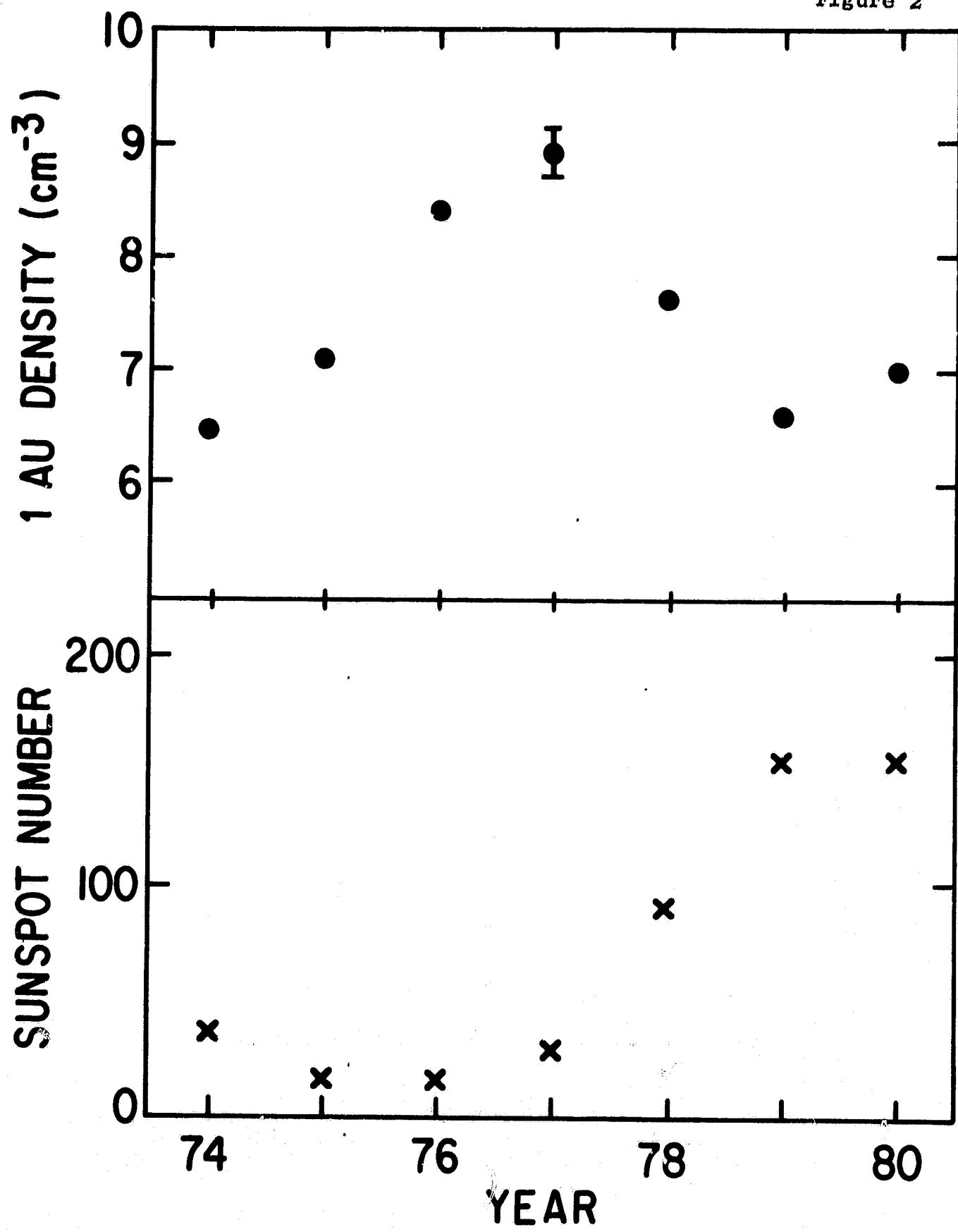


Figure 3

